Optimization of the volume ablation rate for metals at different laser pulse-durations from ps to fs

Beat Neuenschwander*[a], Beat Jaeggi[a], Marc Schmid[a], Vincent Rouffiange[b] and Paul-E. Martin[c]

[a]Bern University of Applied Science, Pestalozzistrasse 20, 3400 Burgdorf, Switzerland
[b]Amplitude Systemes, 11 avenue de Canteranne, Cité de la Photonique, 332600 Pessac, France
[c]Lasea SA, Liège Science Parc, rue des Chasseurs Ardennaise 10, 4031 Angleur, Belgium

ABSTRACT

Ultra short laser pulses in the ps or fs regime are used, when high requirements concerning machining quality are demanded. However, beside the quality also the process efficiency denotes a key factor for the successful transfer of this technology into real industrial applications. Based on the ablation law, holding for ultra short pulses with moderate fluences, it has been shown that the volume ablation rate can be maximized with an optimum setting of the laser parameters. The value of this maximum depends on the threshold fluence and the energy penetration depth. Both measures themselves depend on the pulse duration. For metals the dependence of the threshold fluence is well known, it stays almost constant for pulse durations up to about 10 ps and begin then to slightly increase with the pulse duration. The contrary behavior is observed for the energy penetration depth, it decreases over the whole range when the pulse duration is raised from 500 fs to 50 ps. In this paper we will show that the maximum ablation rate can therefore be increased by a factor of 1.5 to 2 when the pulse duration is reduced from 10 ps down to 500 fs.

Keywords: Ultra short pulses, ablation rates, pulse duration dependency, process optimization, fs, ps

1. INTRODUCTION

In pulsed laser material processing, two different types of laser systems with different regions of pulse durations are currently used. A first large family of pulsed laser systems are Q-switch systems which produce pulse durations in the region of a few to a few tenths of nanoseconds. These types of lasers show relatively high energy per pulse and are quite low cost systems working in the regime of hot ablation (for metals). The second family, the ultra short pulsed systems, work in the cold ablation regime and show clear advantages concerning machining quality, heat affected zone, debris, etc[1-4]. But even if the excellent machining quality is one of the key advantages of ultra short pulsed systems, it may be more cost effective to use a Q-Switched system and to accept the reduced quality and additional costly post processing steps. One possibility to further increase the competitiveness of ultra short pulsed systems may be the change to fiber based amplifier technologies. Without CPA technology the pulse duration of these systems is expected to be in the range of several tens ps[5-7]. For metals the ablation efficiency significantly drops by about a factor of 5 when the pulse duration is raised from 10 ps up to 50 ps[8,9], for nonmetals this drop is be less pronounced but still present[10]. The characteristics of the measured ablation efficiency as a function of the pulse duration implies, that the efficiency could increase when the pulse duration is reduced from 10 ps into the sub ps regime. Results corroborating this belief for metals have been reported[11-13]. For dielectrics and pulse durations reports show an increase of the efficiency for a pulse range from 7 fs – 300 fs[14]. This encourages the development of fiber based ultra short pulsed systems in the fs-regime which can be driven to high average powers by succeeding amplifier stages; recently more than 1kW average power with fs – laser pulses were demonstrated[15,16]. From this point of view sub – ps systems seem to be very attractive for laser micro processing. However, optimizing the process efficiency remains a key factor for the successful transfer of ultra-short pulses into real industrial applications.

*beat.neuenschwander@bfh.ch; phone +41 34 426 42 20; fax +41 34 423 15 13; ti.bfh.ch/alps

2. ABLATION MODEL

2.1 Theory

For ultra short pulses the heat-transfer process in metals is described with the two temperature model[1,17-21] where the temperatures of the electrons and the lattice are treated separately. The results of the model and the experiments show, that the ablation depth z_{abl} can be written as a function of the fluence ϕ_a (pulse energy per unit area):

$$z_{abl} = \delta \cdot \ln\left(\frac{\phi_a}{\phi_{th,a}}\right) \qquad (1)$$

with $\phi_{th,a}$ the threshold fluence and δ the energy penetration depth. Frequently two different ablation regimes are reported[19,22]: firstly the low fluence regime where the optical penetration depth dominates and secondly the high fluence regime where the energy transport is dominated by the heat diffusion of the hot electrons. The two regimes show different threshold fluences and penetration depths whereupon the corresponding values for the second regime are higher.

The logarithmic ablation law is a consequence of an exponential drop of the deposited energy per unit volume with the distance z to the surface and the separation of the energy deposition and the evaporation process. The deposited energy per unit area directly scales with the first derivative of the fluence with respect to z.

$$\frac{dE}{dV}(z) = \frac{1}{\delta} \cdot \phi(z) = \frac{1}{\delta} \cdot \phi_a \cdot e^{-\frac{z}{\delta}} \qquad (2)$$

with ϕ_a the absorbed fluence at the surface. All material is ablated up to a depth where the absorbed energy per unit volume corresponds to about $\rho \cdot \Omega$ (ρ: density; Ω: specific heat of evaporation). Introducing this into (2) directly leads to (1) with a threshold fluence of $\phi_{th,a} = \delta \cdot \rho \cdot \Omega$. Figure 1 shows for a top hat beam the absorbed energy per unit volume and the ablation depth, defined by the threshold fluence, the absorbed fluence ϕ_a and the penetration depth δ. Only the green part p_U of the energy is really used to ablate (evaporate) the material, the red part of the energy, p_L, is lost.
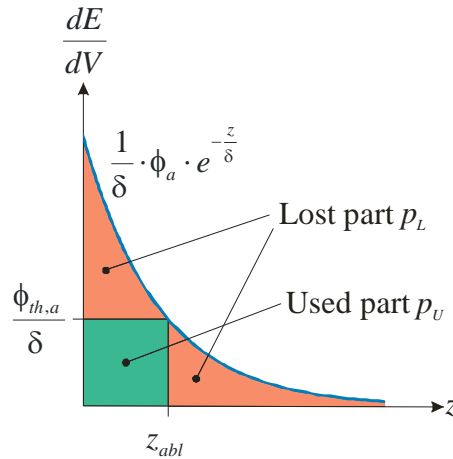

Figure 1. Only the green part of the absorbed energy per unit area is used to evaporate the material. The lost parts are marked in red.

The ratio $\eta = P_U/(P_U+P_L)$ denotes the efficiency of the ablation process and depends on ϕ_a and $\phi_{th,a}$. A short calculation shows that this efficiency is given by

$$\eta = \frac{p_U}{p_U + p_L} = \frac{\phi_{th,a}}{\phi_a} \cdot \ln\left(\frac{\phi_a}{\phi_{th,a}}\right) \qquad (3)$$

and shows a maximum value at

$$\frac{\phi_a}{\phi_{th,a}} = e \tag{4}$$

Introducing (4) into (1) shows, that the maximum efficiency of the ablation process is obtained when the ablation depth z_{abl} per pulse exactly equals the penetration depth of the energy δ. The ablated volume per pulse then reads:

$$\Delta V_{Pulse} = \pi \cdot w_0^2 \cdot \delta \tag{5}$$

The same result as it was obtained by a numerical simulation approach in[23]. It is noted here, that the fluence ϕ_a as well as the threshold fluence $\phi_{th,a}$ denote the absorbed parts where the reflectivity is already taken into account. In real situations the reflectivity of a surface depends on many parameters and is not exactly known. Therefore it is convenient to use the incident fluence $\phi = \phi_a/(1\text{-}R)$ and the threshold $\phi_{th} = \phi_{th,a}/(1\text{-}R)$. The expressions for the logarithmic ablation law (1), the quotient between fluence and threshold (4) and the ablated volume per pulse for a top hat (5) at the maximum efficiency are still valid.

The upper considerations clearly show that for a top hat beam the efficiency of the ablation process can be maximized. At this optimum point the incident fluence is e-times higher than the threshold (4) and the efficiency (3) then amounts 36.8%. Expressions (4) and (5) allow to calculate the maximum volume ablation rate for a top hat beam with average power P_{av}, it amounts $\dot{V}_{max}/P_{av} = 1/e \cdot \delta/\phi_{th}$, the same result as it was obtained in a different way in[25].

2.2 Ablation for a Gaussian beam

For a Gaussian shaped beam, as emitted by most ultra short pulsed systems, the fluence as a function of the distance r to the beam center reads:

$$\phi(r) = \phi_0 \cdot e^{-2 \cdot \frac{r^2}{w_0^2}} \tag{6}$$

Where the peak fluence in the center of the beam ϕ_0

$$\phi_0 = \frac{2 \cdot E_p}{\pi \cdot w_0^2} \tag{7}$$

is given by the pulse energy E_p and the spot radius w_0. The ablated volume per pulse, ΔV, can be calculated by inserting (6) and (7) into (1) and integrating over the ablated area. It reads[24,25]:

$$\Delta V = \frac{1}{4} \cdot \pi \cdot w_0^2 \cdot \delta \cdot \ln^2\left(\frac{\phi_0}{\phi_{th}}\right) \tag{8}$$

For a laser working at a constant average power P and repetition rate f the pulse energy is given by $E_p = P/f$ and the total ablated volume per time amounts:

$$\dot{V} = f \cdot \Delta V \tag{9}$$

Inserting (7) and (8) into (9) lead to:

$$\dot{V} = \frac{1}{4} \cdot \pi \cdot w_0^2 \cdot \delta \cdot f \cdot \ln^2\left(\frac{2 \cdot P}{f \cdot \pi \cdot w_0^2 \cdot \phi_{th}}\right) \tag{10}$$

This expression clearly shows that for a given average power P and spot radius w_0, the volume ablation rate depends on the material parameters ϕ_{th} and δ and the repetition rate f. Figure 2 compares this model (10) with experimental data for Cu-DHP (in US: C12 200).

A very good agreement between the model (10) and the experimental data can be observed. It can also clearly be seen that the volume ablation rate shows a maximum value at an optimum repetition rate. The corresponding values per average power can be calculated from (10):

$$\frac{\dot{V}_{max}}{P_{av}} = \frac{2}{e^2} \cdot \frac{\delta}{\phi_{th}} \tag{11a}$$

$$\frac{f_{opt}}{P_{av}} = \frac{2}{e^2} \cdot \frac{1}{\pi \cdot w_0^2 \cdot \phi_{th}} \tag{11b}$$
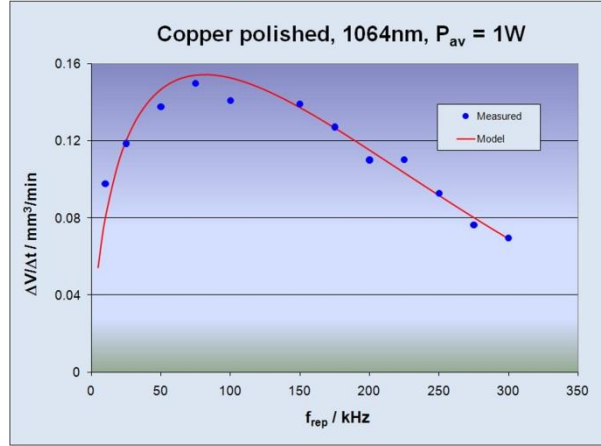

Figure 2: Measured volume ablation rate (blue dots) compared with a least square fit to the model (red solid line) for Cu-DHP.

It is noted here, that also for a Gaussian beam the ablated volume per pulse at its optimum point equals to $\Delta V_{Pulse} = \pi \cdot w_0^2 \cdot \delta$ which is exactly the same result as the one obtained for a top hat beam in the previous section. The maximum volume ablation rate dV_{max}/dt as well as the optimum repetition rate f_{opt} therefore directly scales with the average power. In addition the maximum volume ablation rate per average power only depends on the material parameter ϕ_{th} and δ, i.e. these parameters define the maximum achievable volume ablation rate for a material.

2.3 Incubation

Due to incubation effects the threshold fluence may strongly depend on the number of pulses applied, which is described for metals in[8,9,24,26,27], for semiconductors in[28] and for transparent materials in[29]. The most proposed model to describe the dependency of the threshold fluence on the number of pulses applied is given in[26]:

$$\phi_{th}(N) = \phi_{th,1} \cdot N^{S-1} \tag{12}$$

Where $\phi_{th,1}$ denote the threshold fluence for one pulse and the exponent S denotes the incubation coefficient. For $S = 1$ incubation is absent. But it has to be pointed out that the equation (12) predicts for an infinitive number of pulses that the threshold fluence per pulse becomes zero. From a physically point of view this is not possible. Therefore[29] propose an alternative model:

$$\phi_{th}(N) = \phi_{th,\infty} + (\phi_{th,1} - \phi_{th,\infty}) \cdot e^{-k \cdot (N-1)} \tag{13}$$

Here $\phi_{th,1}$ denotes the single pulse threshold fluence and $\phi_{th,\infty}$ the threshold fluence for an infinite number of pulses. Figure 3 shows on the left the difference between the least square fits to the two models based on measured data from[8,9] for a pulse duration of 10 ps and Cu-DHP. Despite the physical incorrectness of (12) this model seems to better fit the measured values. Similar models can be used for δ and again the fit with a potential function better reproduces the measured values shown in the right side of Figure 3.

Introducing the potential function with the incubation coefficients S_ϕ for the fluence and S_δ for the penetration depth, the maximum volume ablation rate (11a) reads:

$$\frac{\dot{V}_{max}}{P_{av}} = \frac{2}{e^2} \cdot \frac{\delta_1}{\phi_{th,1}} \cdot N^{S_\delta - S_\phi} \tag{14}$$

For metals both incubation coefficients do not strongly differ and the maximum volume ablation rate is only minor influenced by the number of pulses applied even when the threshold and the penetration depth may significantly change.
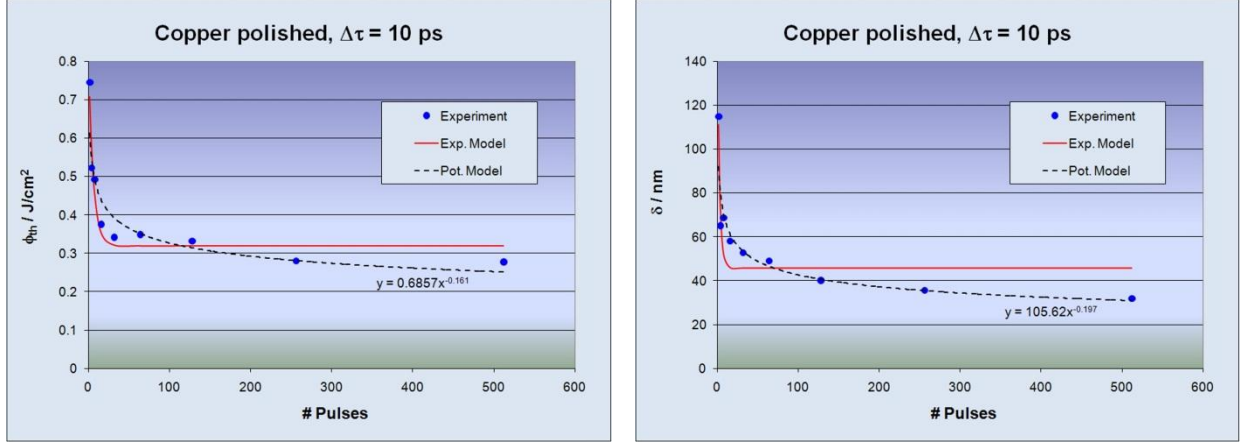

Figure 3: left: Threshold fluence ϕ_{th} as function of the number of pulses applied and corresponding least square fits with the two models. Right: Penetration depth δ as function of the number of pulses applied and corresponding least square fits with the two models.

2.4 Consequences

The considerations in the previous sections clearly show that the ablation process can be optimized and that the maximum volume ablation rate is finally given by the threshold fluence ϕ_{th} and the energy penetration depth δ. For metals and pulses longer than 10 ps the threshold fluence begins to increase[8,9,10,19]. But beside the threshold fluence also the penetration depth δ has an influence onto the maximum volume ablation rate. For pulse durations in the range from 10 ps to 50 ps it is shown that the value of δ decreases with increasing pulse duration[8,9,10,19]. Therefore the maximum volume ablation rate and the ablation efficiency in general drops significantly when the pulse duration is raised from 10 ps to 50 ps. The situation changes for shorter pulses. In metals the time for the energy transfer from the free electrons to the lattice, the electron-phonon thermalization time, amounts a few ps[3,30]. A further reduction of the pulse duration will not lead to additional benefits in terms of the threshold fluence ϕ_{th}[2,3,30] which would stay constant. If shorter pulses should lead to higher ablation rates this could only be caused by a higher penetration depth δ for shorter pulses. This will be investigated in the following sections for pulse durations from 500 fs up to 10 ps for copper, steel, brass and undoped silicon.

An additional remark has to be placed here: Often in the literature two or more different situations are compared, e.g. different materials, pulse durations, wavelengths etc. Mostly this is done with identical parameters as repetition rate, focus radius and pulse energy. But one has to have in mind that the efficiency of the ablation process is strongly influenced by the threshold fluence and the penetration depth and that these two measures depend on many parameters as seen above. Figure 4 shows the volume ablation rate for two different sets of ϕ_{th} and δ for an average power of 1 W and a spot radius of 20 μm. If the ablation rates are compared e.g. at equal repetition rates the blue curve will dominate up to about 200 kHz and afterwards the red curve will be the more efficient one i.e. depending on the chosen repetition rate one set of parameters can be more efficient than the other and vice versa. This might be a cause that sometimes contradictory results concerning the ablation rates are reported in the literature. It becomes clear, that a fair comparison between different situations should be done by deducing the maximum ablation rate. This can be realized by experimentally deducing the threshold fluence and the penetration depth.
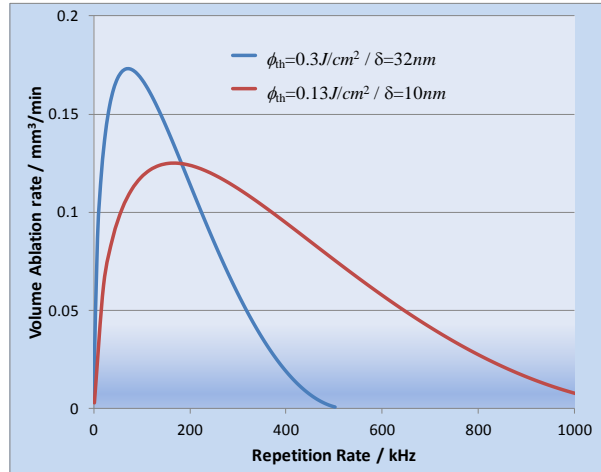
Figure 4: Volume ablation rate for an average power of 1 W, a spot radius of 20μm for two different sets of ϕ_{th} and δ.

3. EXPERIMENTAL SET UP

The experimental set up is shown in figure 5. The laser system was a SATSUMA (Amplitude Systemes, France) fs-laser working at a wavelength of 1030 nm with pulse duration between 500 fs and 10 ps set up in a MOPA arrangement. The pulse duration can be changed from 500 fs to higher values by detuning the pulse compressor. The pulse duration was deduced with an autcorrelator whenever the pulse duration was changed. An additional modulator, introduced after the last amplifier stage, served as a pulse on demand (POD) option. The beam is guided through 3 folding mirrors and a quarter wave plate, to generate a circular polarized beam, onto a fourth folding mirror into a LASEA machining head. In the machining head the beam passes a folding mirror followed by a 2-lens beam expander and a two lens focus shifter. Finally two galvo mirrors guide the beam through an f-theta-objective onto the work piece. The whole processing head could be automatically adjusted in z-direction in order to have the focal plane on the work piece. The spot size and the beam quality were measured with a rotating slit beam profiler. Due to the small beam radius the second moment analysis method showed too high values of the spot radius and beam quality factor M^2. Therefore a second measurement was taken with a Gauss-fit analysis. Both measurements were made with 0° and 45° axis orientation of the beam profiler. The geometric mean value of all measurements is used as spot radius and beam quality factor. The measured values were $w_0 = 13.5$ μm and $M^2 = 2$, i.e. the beam was not exactly Gaussian shaped but is treated like one for the analysis of the results. The transmission through the whole optical path with bending mirrors and lenses amounted 69%.

In order to deduce ϕ_{th} and δ as a function of the pulse duration and the number of pulses applied, series with single ablated craters were generated for each set of these parameters, i e. 1,2,4,...,512 pulses and 500 fs, 800 fs, 2 ps, 3 ps, 5 ps and 10 ps. For one series the pulse energy was raised from below up to multiples of the threshold. To avoid thermal accumulation effects the repetition rate was set to 1 kHz with the POD. The crater depths in the centre were deduced with a laser scanning microscope. These results were compared with the theoretical crater depth by introducing the peak fluence (7) into (1). The two parameters ϕ_{th} and δ were then deduced by a least square fit. This analysis was done for copper, steel, brass and undoped silicon. Especially at low pulse energies i.e. low fluences or low number of pulses applied the deduction of the crater depth became extensive and sometimes almost impossible. On the other side, too high fluences and pulse numbers lead to deep craters where it was no longer possible to measure the depth in the center. The deduction of the threshold fluence with the squared diameter as e.g. done in[28] would overcome this drawbacks but wouldn't give any information about the penetration depth δ which is necessary to deduce the maximum volume ablation rate according to (11a). Due to the limited data the incubation effect could not really by analyzed in the investigated pulse duration regime and will be subject of future investigations.

The volume ablation rate can also be determined by marking straight lines. Here different repetition rates, marking speeds and repeats could be chosen. The number of pulses applied can be estimated by the spot diameter, repetition rate, marking speed and number of repeats. The volume ablation rate can then be deduced by measuring the ablated volume of a line segment with the laser scanning microscope. Together with the marking speed, the length of the segment and the

number of repeats the volume ablation rate can exactly be calculated. By marking lines at constant average power, repetition rate and marking speed the volume ablation rate can directly be compared for different pulse durations.. Nevertheless straight lines were marked for the investigated materials copper, steal, brass and undoped silicon. For copper and steel the results are compare with the obtained for longer pulse durations up to 50 ps from previous works[8-10] with a DUETTO (time-bandwidth products) ps-system.
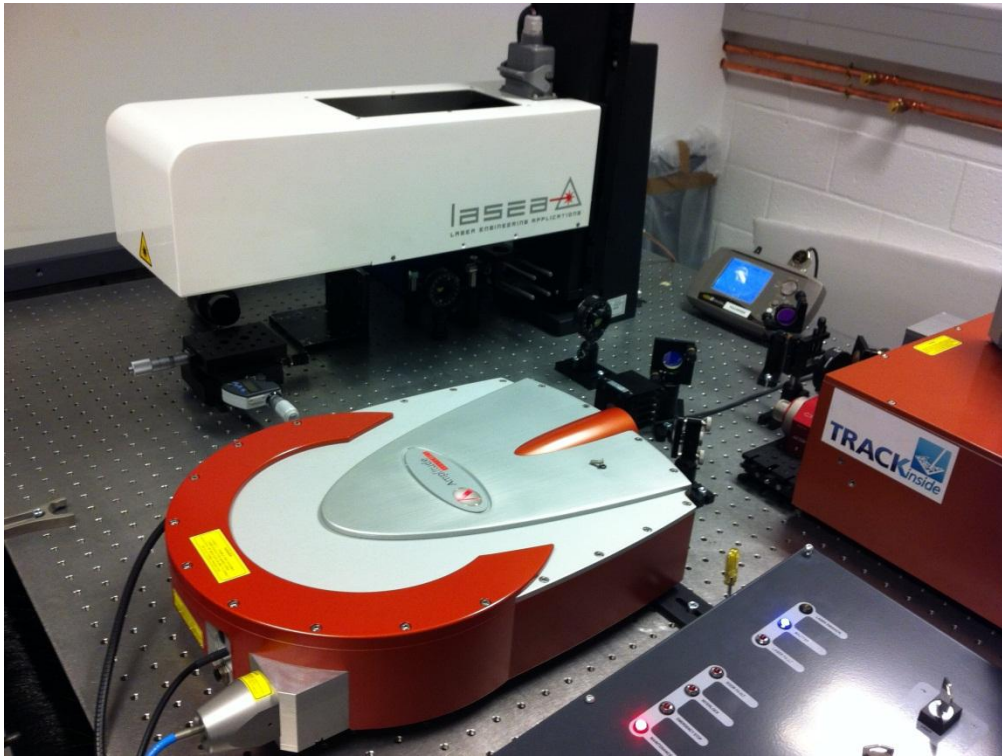
Figure 5: Picture from the experimental set up.

4. EXPERIMENTAL RESULTS

4.1 Copper

For copper the ablation study was performed with peak fluences (7) between 0.06 J/cm^2 and 2 J/cm^2. The results for 128, 64 and 32 pulses could be fully analyzed for all pulse durations. The obtained results for 128 pulses are summarized with red dots in figure 6. For comparison the results for longer ps-pulses from[8-10] are added with blue triangles. On the right side it can be clearly seen, that for the pulse duration of 800 fs up to 10 ps the threshold fluence almost rests unchanged as expected[30], the small variations lie within the measurement uncertainty. The value measured for 10 *ps* from the SATSUMA experiments also fits the value obtained from the former experiments with the DUETTO system. The penetration depth δ is shown in the middle. The penetration depth raise from about 15 nm at 50 ps up to about 75 nm when the pulse duration decreases to 500 fs. This value corresponds very well with the thermal diffusion length of the electrons as it was observed for copper with a pulse duration of 150 *fs* and wavelength of 800 nm in[19]. Due to this behavior of the penetration depth the maximum volume ablation rate increases by about 75% from 0.2 $mm^3/min/W$ at 10 ps pulse duration up to about 0.35 $mm^3/min/W$ for 500 fs. In[13] the volume ablation rates were deduced for different materials by marking straight lines. There a maximum value 0.21 $mm^3/min/W$ for a pulse duration of 900 fs was obtained.

With the marked lines an increase of the volume ablation rates of about 50% was observed. Figure 7 shows SEM pictures of marked lines at 10 ps and 500 fs pulse duration, marking speed of 160 mm/s with 8 repeats generated at 370 mW average power (on the target surface) and a repetition rate of 100 kHz. There is no significant difference in the

surface quality observed between to two pulse durations. The situation slightly changes when the ablated craters are analysed. Figure 8 shows the ablated craters produced with a peak fluence of 0.4 J/cm^2 and with 256 pulses for 10 ps, 2 ps and 500 fs pulse duration. The small "worms" of melted material indicate that it was worked in the regime dominated by the thermal diffusion of the hot electrons. It can clearly be seen that for shorter pulse duration this melting effects are reduced and that the crater becomes bigger and deeper as well.
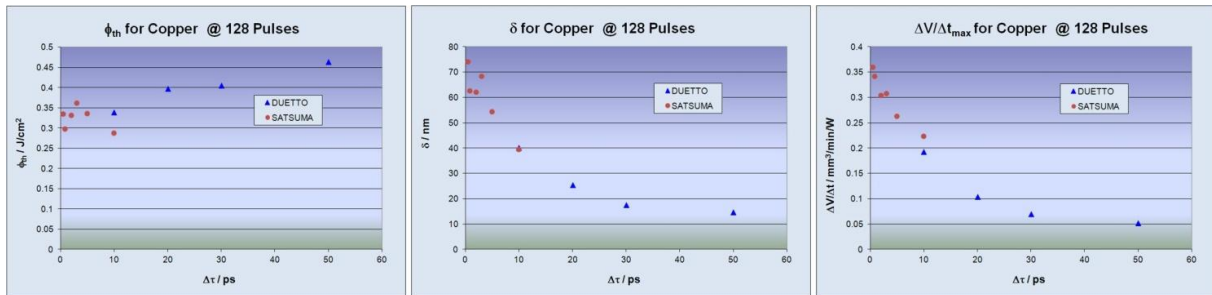
Figure 6: Threshold fluence, penetration depth and maximum volume ablation rate between 500 fs and 10 ps (red circles) and from 10 ps to 50 ps (blue triangles) for copper and 128 pulses
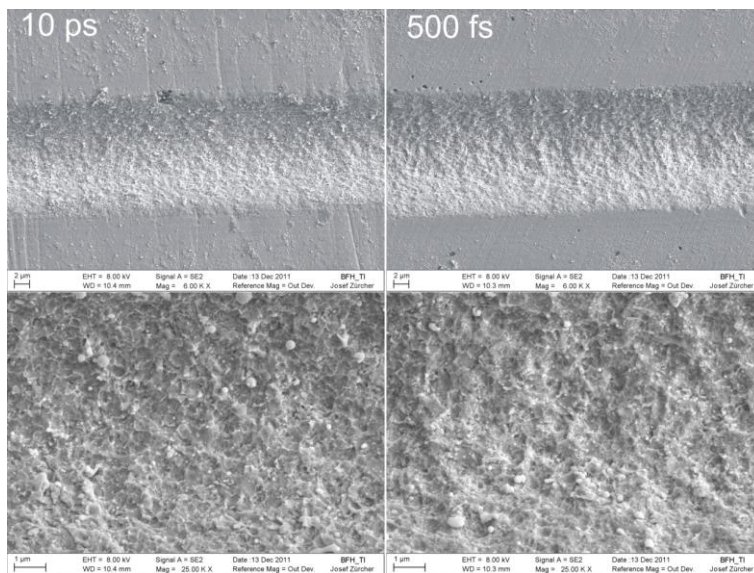
Figure 7: SEM images with detail view of marked lines in copper with 8 repeats. The average power was 370 mW at a repetition rate of 100 kHz corresponding to a peak fluence of 1.3 J/cm^2. The marking speed amounted 160 mm/s.
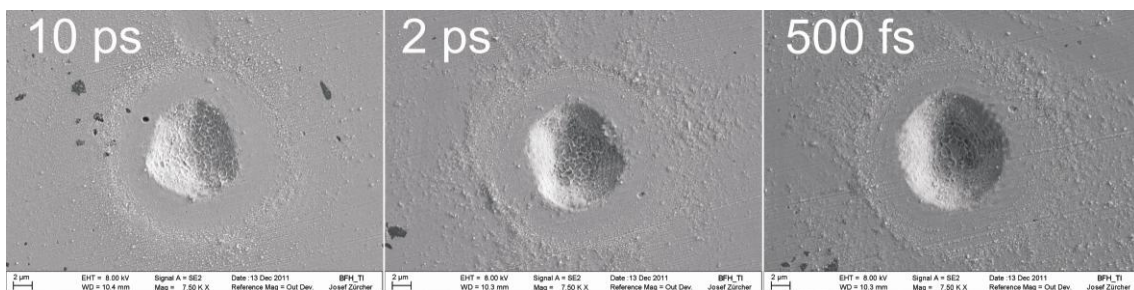

Figure 8: Ablated craters in copper with a peak fluence of 0.4 J/cm^2 and 128 pulses applied.

4.2 Steel

For steel the results for 256, 128 and 64 pulses could be fully analyzed for all pulse durations. The results for 256 pulses applied are summarized in figure 9. In principal the behavior of the threshold fluence and the penetration depth do not

differ from the one for copper. Also here the threshold fluence rests unchanged for pulses shorter than 10 ps and the penetration depth increases for shorter pulses. The maximum volume ablation rate again increases by about 75% to a value of 0.4 mm^3/min/W when the pulse duration is reduced from 10 ps to 500 fs.
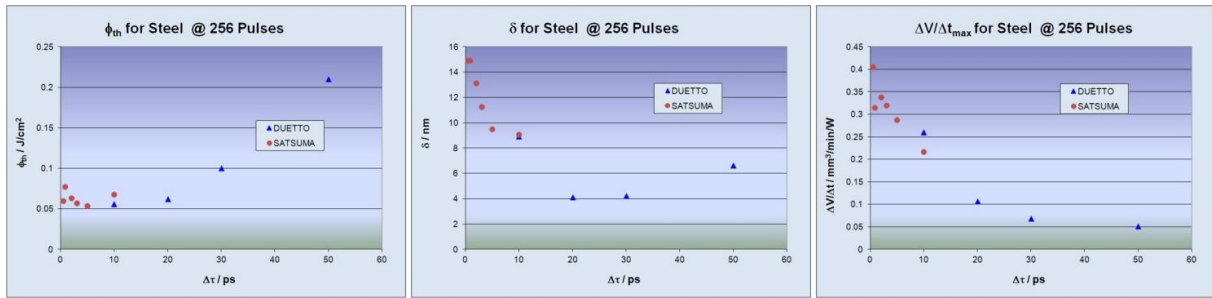
Figure 9: Threshold fluence, penetration depth and maximum volume ablation rate between 500 fs and 10 ps (red circles) and from 10 ps to 50 ps (blue triangles) for steel and 256 pulses.
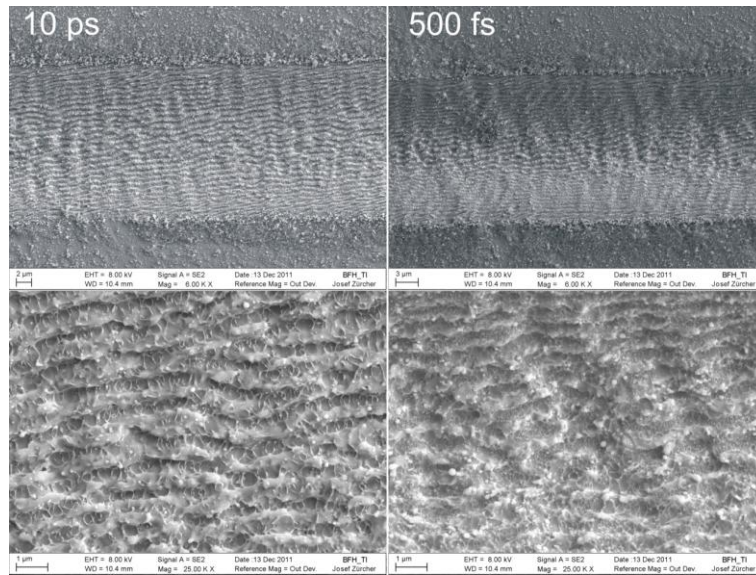

Figure 10: SEM images with detail view of marked lines in copper with 15 repeats. The average power was 170 mW at a repetition rate of 100 kHz corresponding to a peak fluence of 0.63 J/cm^2. The marking speed amounted 160 mm/s.

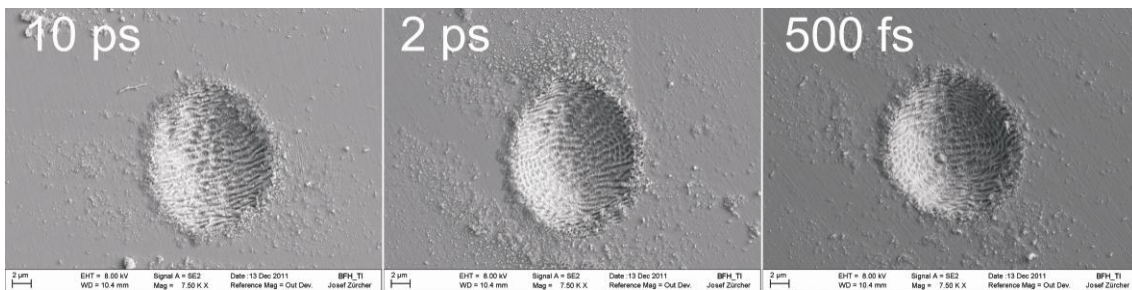Figure 11: Ablated craters in steel with a peak fluence of 0.2 J/cm^2 and 256 pulses applied.

Figure 10 shows the SEM image with detail view of lines marked with an average power of 170 mW at a repetition rate of 100 kHz with a making speed of 160 mm/s and 15 repeats. Please note that the scale for the upper images differs for 10 ps and 500 fs and the apparent smaller line width for 500 fs is due to this different scale. In the lower detail view small "worms of melted material" are observed between the ripples. These "worms" are much less pronounced for the pulse duration of 500 fs. The orientation of the ripples is due to the circular polarization state[31].

The SEM images of ablated craters are shown for 10 ps, 2ps and 500 fs in Figure 11. The craters were generated with 256 pulses and with a peak fluence of 0.2 J/cm^2. Due to the lower threshold the crater diameter are bigger compared to the ones for copper in figure 8. Again ripples are observed, but no "worms" of melted material can be seen. This may be due to the 3 times lower peak fluence compared to the one used for the marked lines in figure 10. The depth of the craters increase with decreasing pulse duration i.e. the ablation becomes more efficient but no significant difference in the surface quality can be seen.

4.3 Brass

For brass the results for 128, 64, 32 and 16 pulses could be fully analyzed for all pulse durations from 500 fs up to 10 ps. The results for 128 pulses applied are summarized in figure 12. No measurements for the pulse duration regime between 10 ps and 50 ps were done in previous work. Again the threshold fluence rests almost unchanged for the investigated range of pulse durations. Also the penetration depth increases with shorter pulses, this increase is much less pronounced compared to copper and steel. Therefore even though the gain in the maximum volume ablation rate is reduced, it still amounts about 40% when the pulse duration is decreased from 10 ps to 500 fs.
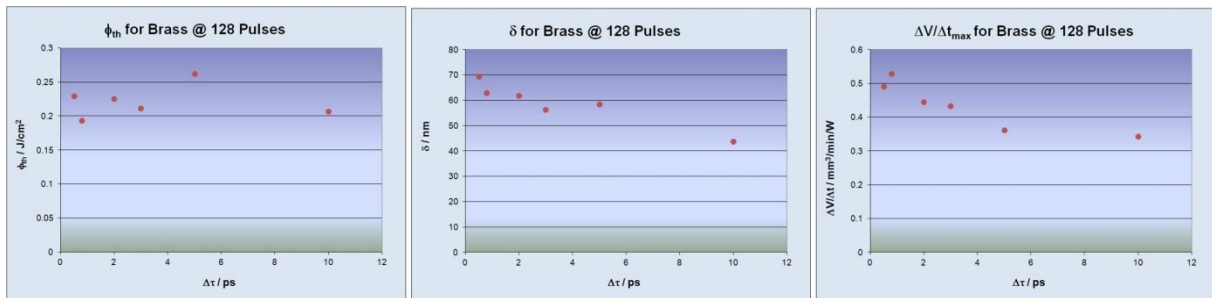

Figure 12: Threshold fluence, penetration depth and maximum volume ablation rate between 500 fs and 10 ps for brass and 128 pulses.

4.4 Undoped Silicon

For undoped silicon only the results for 32 and 16 pulses could be fully analyzed for all pulse durations from 500 fs up to 10 ps. The results for 64 pulses applied are summarized in figure 13. Again the threshold fluence rests almost stable for the investigated range of pulse durations but the penetration depth increases from 40 nm at 10 ps pulse duration up to more than 90 nm for the pulse duration of 500 fs. With this the maximum volume ablation rate is more than doubled for the shortest pulses compared to 10 ps. As reported in[10] also here crater and cone formation is observed. This is shown in figure 14 for craters ablated with 64 pulses at a peak fluence of 0.57 J/cm^2 and in figure 15 for lines marked with a speed of 320 mm/s at an average power of 350 mW and a repetition rate of 71 kHz with 64 repeats. For a pulse duration of 10 ps melting effects are observed for the craters and the lines as well. These effects are much reduced for 500 fs pulses but there, especially for the marked lines, small and deep craters appear. It can be seen from figure 15 that this crater formation already begins at 10 ps pulse duration but the number of craters is less and its depth is much smaller.
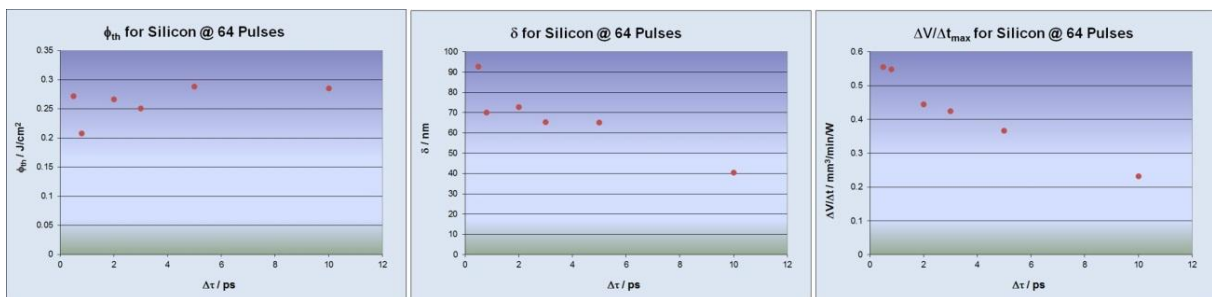

Figure 13: Threshold fluence, penetration depth and maximum volume ablation rate between 500 fs and 10 ps for silicon and 64 pulses.
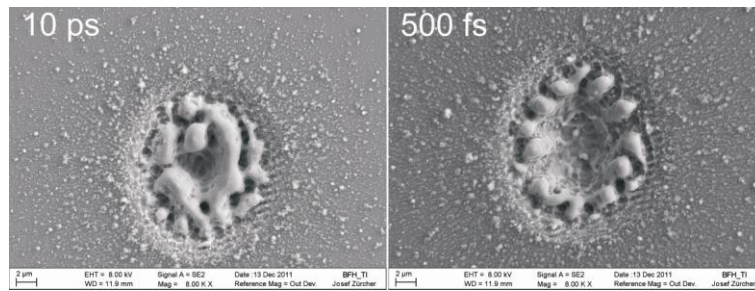
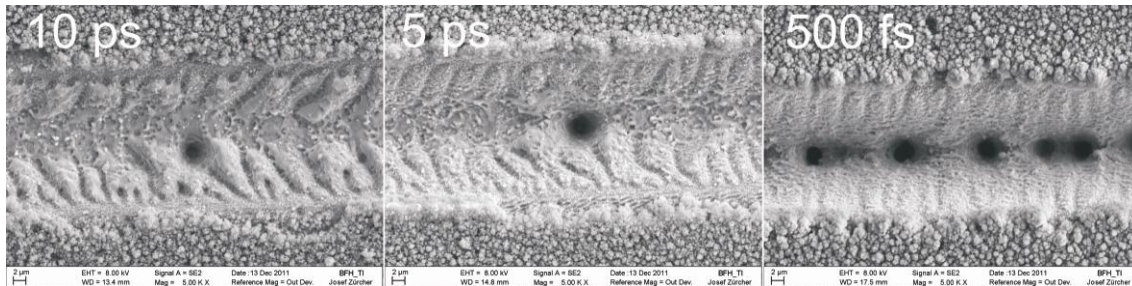Figure 14: Ablated craters in undoped silicon with a peak fluence of 0.57 J/cm^2 and 64 pulses applied.

Figure 15: SEM images of marked lines in undoped silicon with 64 repeats. The average power was 350 mW at a repetition rate of 71 kHz corresponding to a peak fluence of 1.73 J/cm^2. The marking speed amounted 320 mm/s.

5. CONCLUSIONS

It has been shown that with the proper value of the applied fluence compared to the threshold fluence the process efficiency of ultra short pulsed laser ablation can be maximized. The maximum value of the ablated volume per time and average power scales directly with the energy penetration depth and the inverse of the threshold fluence. Due to incubation these two values strongly depend on the number of pulses applied at the same position. If the two incubations coefficients for the threshold fluence and the penetrations depth strongly differ, then the maximum ablation rate will also strongly depend on the number of pulses applied. Beside the number of pulses the threshold fluence and the penetration depth depend on the pulse duration as well. As expected the threshold fluence will only change very slightly if the pulse duration is decreased from 10 ps to 500 fs. In contrast the energy penetration depth can strongly increase for shorter pulses. This finally leads to an increased volume ablation rate for shorter pulses. The gain in efficiency which can be realized by the reduction of the pulse duration from 10 ps down to 500 fs depends on the material, here it amounted 75% for copper and steel, 40% for brass and more than 100% for undoped silicon. The obtained results clearly show that the ablation efficiency can be improved by a factor up to 2 when the pulse duration is decreased from 10 ps to 500 fs, furthermore melting effects, appearing at 10 ps, can be reduced, as well. From this point of view, shorter pulses could be a possibility to increase the competitiveness of ultra short pulsed laser systems for laser micro processing.

6. ACKNOWLEDGEMENTS

REFERENCES

[1] B. N. Chichkov, C. Momma, S. Nolte, F. von Alvensleben and A. Tünnermann, „Femtosecond, picosecond and nanosecond laser ablation of solids", Appl. Phys. A 63, 109 (1996).

[2] Detlef Breitling, Andreas Ruf and Friedrich Dausinger, "Fundamental aspects in machining of metals with short and ulrashort laser pulses", Proc. SPIE 5339, 49-63 (2004)

[3] Friedrich Dausinger, Helmut Hügel and Vitali Konov, "Micro-machining with ultrashort laser pulses: From basic understanding to technical applications", Proc. SPIE Vol. 5147, 106-115 (2003)

[4] J. Meijer, K. Du, A. Gillner, D. Hoffmann, V. S. Kovalenko, T. Masuzawa, A. Ostendorf, R. Poprawe, W. Schulz, "Laser Machining by Short and Ultrashort Pulses – State of the Art", Annals of the CIRP, 51/2 (2002)

[5] S. Pierrot, J. Saby, B. Cocquelin and F. Salin, "High-Power all Fiber Picosecond Sources from IR to UV", Proc. of SPIE Vol. 7914, paper 79140Q (2011)

[6] S. Kanzelmeyer, H. Sayinc, T. Theeg, M. Frede, J. Neumann and D. Kracht, "All-fiber based amplification of 40 ps pulses from a gain-switched laser diode", Proc. of SPIE Vol. 7914, paper 191411 (2011)

[7] P Deladurantaye, A. Cournoyer, M. Drolet, L. Desbiens, D. Lemieux, M. Briand and Y. Taillon, "Material micomachining using bursts of high repetition rate picoseconds pulses from a fiber laser source", Proc. of SPIE Vol. 7914, paper 791404 (2011)

[8] M. Schmid, B. Neuenschwander, V. Romano, B. Jaeggi and U. Hunziker, "Processing of metals with ps-laser pulses in the range between 10ps and 100ps", Proc. of SPIE Vol. 7920, paper 792009 (2011)

[9] B. Jaeggi, B. Neuenschwander, M. Schmid, M. Muralt, J. Zuercher and U. Hunziker, "Influence of the Pulse Duration in the ps-Regime on the Ablation Efficiency of Metals", Physics Procedia 12, 164-171 (2011)

[10] B. Neuenschwander, B. Jaeggi, M. Schmid, U. Hunziker, B. Luescher, C. Nocera, "Processing of industrially relevant non metals with laser pulses in the range between 10 ps and 50 ps", ICALEO 2011, Paper M103 (2011)

[11] B. Sallé, O. Gobert, P. Meynadier, G. Petite and A. Semerok, "Femtosecond and picosecond laser microablation: ablation efficiency and laser microplasma expansion", Appl. Phys. A 69[Suppl.], 382 – 383 (1999)

[12] R. Le Harzig, D. Breitling, M. Weikert, S. Sommer, C. Föhl, S. Valette, C. Donnet, E. AUdouard and F. Dausinger, "Pulse width and energy influence on laser micromachining of metals in a range of 100 fs to 5 ps", Appl. Surf. Science 249, 322-331 (2005)

[13] J. Lopez, A. Lidolff, M. Delaigue, C. Hönninger, S. Ricaud and E. Mottay, "Ultrafast Laser with highEnergy and high average power for Industrial Micromachining: Comparision ps-fs", ICALEO 2011, Paper 401 (2011)

[14] O. Utéza, N. Scanner, B. CVhimier, M. Sentis, P. Lassonde, F. Légardé and J.C. Kieffer, "Surface Ablation od Dielectrics with sub-10 fs to 300 fs Laser Pulses : Crater Depth and Diameter, and Efficiency as a Function of Laser Intensity", JLMN-J. of Laser Micro/Nanoengineering, Vol. 5, No. 3, 238-241 (2010)

[15] P. Russbueldt, T. Mans, J. Weitenberg, H.-D. Hoffmann, R. Poprawe, "Compact diode-pumped 1.1 kW Yb:YAG Innoslab femtosecond amplifier," Opt. Lett. 35, 4169-4171 (2010)

[16] P. Russbueldt, T. Mans, H-D. Hoffmann, R. Poprawe, "1100 W Yb:YAG femtosecond Innoslab amplifier", Proc. of SPIE, 7912 (2011)

[17] C. Momma, B.N. Chichkov, S. Nolte, F. van Alvensleben, A. Tünnermann, H. Welling and B. Wellegehausen, "Short-pulse laser ablation of solid targets", Opt. Comm. 129, 134-142 (1996)

[18] C. Momma, S. Nolte, B.N. Chichkov, F. van Alvensleben and A. Tünnermann, "Precise laser ablation with ultrashort pulses", Appl. Surf. Science 109/110, 15-19 (1997)

[19] S. Nolte, C. Momma, H. Jacobs, A. Tünnermann, B.N. Chichkov, B. Wellegehausen and H. Welling, "Ablation of metals by ultrashort laser pulses", J. Opt. Soc. Am. B, Vol. 14, No. 10 (1997)

[20] S.I. Anisimov and B. Rethfeld, "On the theory of ultrashort laser pulse interaction with a metal", Proc. SPIE 3093, 192-203 (1997)

[21] B.H. Christensen, K. Vestentofrt and P. Balling, "Short-pulse ablation rates and the two-temperature model", Appl. Surf. Science 253, 6347-6352 (2007)

[22] P. Mannion, J. Magee. E. Coyne and G.M. O'Conner, "Ablation Thresholds in ultrafast laser micro-machining of common metals in air", Proc. of SPIE vol. 4876, 470-478 (2002)

[23] G. Hennig, S. Bruening, and B. Neuenschwander, "Laser Microstructuring and Processing in Printing Industry", CLEO:2011 - Laser Applications to Photonic Applications, OSA Technical Digest (CD), paper AMD4 (2011)

[24] G. Raciukaitis, M. Brikas, P. Gecys, B. Voisiat, M. Gedvilas, "Use of High Repetition Rate and High Power Lasers in Microfabrication: How to keep Efficiency High?", JLMN Journal of Laser Micro/Nanoengineering, Vol. 4 (3), 186-191 (2009)

[25] B. Neuenschwander, G. Bucher, C. Nussbaum, B. Joss, M. Muralt, U. Hunziker et al., "Processing of dielectric materials and metals with ps-laserpulses: results, strategies limitations and needs", Proceedings of SPIE vol. 7584, (2010)

[26] Y. Jee, M.F. Becker and R.M. Walser, "Laser-induced damage on single-crystal metal surfaces", J. Opt. Soc. Am. B5, (1988)

[27] P.T. Mannion, J. Magee, E. Coyne, G.M. O'Connor and T.J. Glynn, "The effect of damage accumulation behavior on ablation thresholds and damage morphology in ultrafast laser micro-machining of common metals in air", Appl. Surface Science 233, 275 – 287 (2004)

[28] J. Bonse, J.M. Wrobel, J. Krüger and W. Kautek, "Ultrashort-pulse laser ablation of indium phosphide in air", Appl. Phys. A; Vol. 72, 89 – 94 (2001)

[29] A. Rosenfeld, M. Lorenz, R. Stoian and D. Ashkenasi, "Ulrashort-laser-pulse damage threshold of transparent materials and the role of incubation", Appl. Phys. A; Vol. 69 [Suppl.], 373 – 376 (1999)

[30] G. Mourou et al., "Method for controlling Configuration of laser induced breakdown and ablation", US Patent US RE37,585 E (2002)

[31] B.Tan and K. Venkatakrishnan, "A femtosecond laser-induced periodical surface structureon crystalline silicon", J. Micromech. Microeng. 16, 1-6 (2006)